WAVES–IN–ICE: WAVE ATTENUATION AND ICE BREAKUP

Alessandro Toffoli (1,2) and Jaak Monbaliu (1)

(1) KU Leuven, Belgium, E-mail: toffoli.alessandro@gmail.com and jaak.monbaliu@kuleuven.be
(2) The University of Melbourne, Australia, E-mail: alessandro.toffoli@unimelb.edu.au

A small scale waves-in-ice flume is used to conduct a pilot project to investigate the hydroelastic interactions between water waves of different periods and amplitudes and freshwater floating ice. It is shown that only incident waves with long period and large amplitudes can break up the ice cover and that the extent of the break up increases with increasing period and amplitude. The proportion of the incident wave that propagates through the ice-covered water grows as the period and amplitude increase, indicating the existence of a positive feedback loop between ice break up and increased wave propagation. Results are limited by the brittle nature of the fresh water ice, which is more fragile than sea ice, and the small dimensions of the flume. To achieve a more comprehensive insight of the waves-in-ice problem, an experimental model is planned in a substantially larger wave facility with feature-controlled sea ice model in the wave-ice tank of Aalto University, within the framework of Hydralab+.

1. INTRODUCTION

Sea ice acts as a refrigerator for the world. Its bright surface reflects solar heat, which would otherwise be absorbed by the dark ocean it conceals, and the salt it expels during the freezing process drives thermohaline circulation, which transports cold water towards the equator. As a result, sea ice plays a crucial role in our climate system.

Waves penetrate deep into the ice-covered ocean and impact the ice cover (e.g. Liu and Mollo-Christensen, 1988). Concomitantly, the ice cover attenuates the wave energy over distance, so that wave impacts die out eventually (e.g. Wadhams et al., 1988). The most heralded effect is the ability of waves to break up the ice cover into floes with diameters comparable to the prevailing wavelengths. Asplin et al. (e.g. 2012) report wave-induced breakup 250 km into the Beaufort Sea; Kohout et al. (2014) observed breakup events over 300km into the Antarctic sea ice. The resulting region covered by broken floes, which sits between the open ocean and the quasi-continuous pack ice, is known as the marginal ice zone (MIZ). Following the breakup, waves herd floes (Wadhams, 1983), introduce warm water and overwash the floes, thus accelerating ice melt (Wadhams et al., 1979), and cause the floes to collide, which erodes the floes and influences the large-scale deformation of the ice field via momentum transfer (Shen et al., 1987). Waves, therefore, have a substantial role in controlling the ice extent.

Accounts of wave-induced breakup in the literature are serendipitous and rarely accompanied by data, due to the difficulties in making measurements in the harsh and dynamic MIZ conditions. Models of ice breakup, which are based on strains imposed by waves exceeding a specified failure strain, are embedded into operational climate models (e.g. Williams et al., 2013, and reference therein). These further include the crucial process of wave energy attenuation over distance due to the presence of ice cover. Attenuation dictates the spatial distribution of wave energy in the ice-covered ocean, and hence the region susceptible to breakup. Therefore, an accurate model of attenuation undergirds breakup models and, in turn, climate models.

A series of pioneering experiments were conducted in the Arctic Ocean in the 1970s to early 1980s (e.g. Wadhams et al., 1988). The experiments were a catalyst for development of mathematical attenuation models. The models are conventionally based on an accumulation of scattering events (e.g. Masson and LeBlond, 1989) and/or parameterised viscous dissipation (e.g. Wang and Shen, 2010). Notably, they are also based on linear theories, i.e. the attenuation rate is independent of wave amplitude. Field observations (Kohout et al., 2014) confirm a linear regime exists for attenuation of small-amplitude waves. However, there is a transition in attenuation rates as wave amplitude increases (this is substantiated by a number of field and

laboratory experiments, see e.g. Meylan et al., 2014; Bennetts et al., 2015; Bennetts and Williams, 2015). Thus, the linear model is inaccurate for large-amplitude waves (Toffoli et al., 2015), and, consequently, erroneously predicts wave-induced breakup by up to hundreds of kilometres.

Field experiments are dominated by the natural environment and thus no control is possible, leaving a number of open questions in the interpretation of observations. Laboratory experiments, on the other hand, offer a controlled environment. However, previous tests have been limited to wave attenuation as induced by plastic or wooden plates (e.g. Bennetts and Williams, 2015; Bennetts et al., 2015; Toffoli et al., 2015) due to the difficulties to access proper ice tank facilities. Current knowledge of waves-in-ice is therefore impaired by a backdrop of uncertainties. Here we describe a first attempt to investigate experimentally the interaction between waves and real ice. Results are used to plan a larger scale experiment in the wave-ice tank at Aalto University.

2. A PHYSICAL MODEL IN A SMALL SCALE WAVE-ICE FLUME

Preliminary laboratory experiments were undertaken at the University of Melbourne in a facility consisting of a wave flume housed inside a refrigerated chamber, where air temperatures can be reduced to −15 ˚C (figure 1). The flume is made out of glass supported by a wooden frame, ensuring optical access and that the structure experiences minimal contraction or expansion during freezing and defrosting. The flume is 14 m long, is 0.76 m wide, and was filled with fresh water 0.45 m deep. It is bounded at one end by a computer-controlled cylindrical wave-maker and at the opposite end by a linear beach with slope 1:6, which absorbs incoming wave energy (95% energy-effective for waves tested).

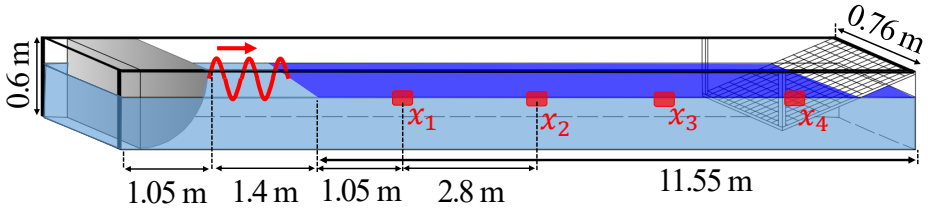

Figure 1: Schematic of the wave flume. The light-blue is the water, and the dark blue is the ice cover. Red rectangles indicate the camera locations.

Regular incident wave fields were generated with different periods, T = 0.8, 1, and 1.2 s (corresponding wavelengths λ = 1, 1.56, and 2.1 m), and amplitudes, a, so that the wave steepness ka = 0.04, 0.06, and 0.1, where k = 2π/λ is the wavenumber. For each incident wave, a floating ice cover was grown, beginning with the water temperature being reduced to 0 ˚C by keeping the air temperature at −1 ˚C for 24 h. The freezing process was then initiated by dropping the air temperature to −12 ˚C for 5 h, at the end of which the ice cover was ≈0.01 m thick and covered the water surface along the full flume length. Tests were executed at an air temperature of −1 ˚C. To allow wave generation in open water, ice in the initial 1.4 m of the flume was removed. With the ice at the desired initial condition, the wave maker was used to generate the specified wave field for 60 s (including a 5 s run-up). In all tests, the incident waves forced a layer of water 3 to 50 mm deep onto the surface of the ice at the leading ice edge (this is normally known as overwash, Nelli et al, 2017). Four cameras with a sampling rate of 60 Hz and a resolution of 1280 × 720 pixels were deployed at distances x_1 = 1.05m, x_2 = 3.85m, x_3 = 6.65m, and x_4 = 9.45 m from the wave maker. An image processing technique was used to extract the oscillatory vertical displacements of the surface (water or ice) in contact with air. Ice displacements were also recorded by tracking red markers embedded in the ice. Note that both techniques return the same displacements in the absence of overwash, while differences are notable in presence of an overwash flow on top of the ice cover.

3. ICE BREAK UP AND WAVE ATTENUATION

Figure 2 shows the amplitudes corresponding to the displacements obtained from the image processing and markers, denoted as a_{im} and a_{mk}, respectively, normalised with respect to the incident wave amplitude, a_0, as measured in the absence of ice. It also shows the ice configuration (broken/unbroken) at the end of each test. A more detailed description of this experiment can be found in Dolatshah et al. (2018).

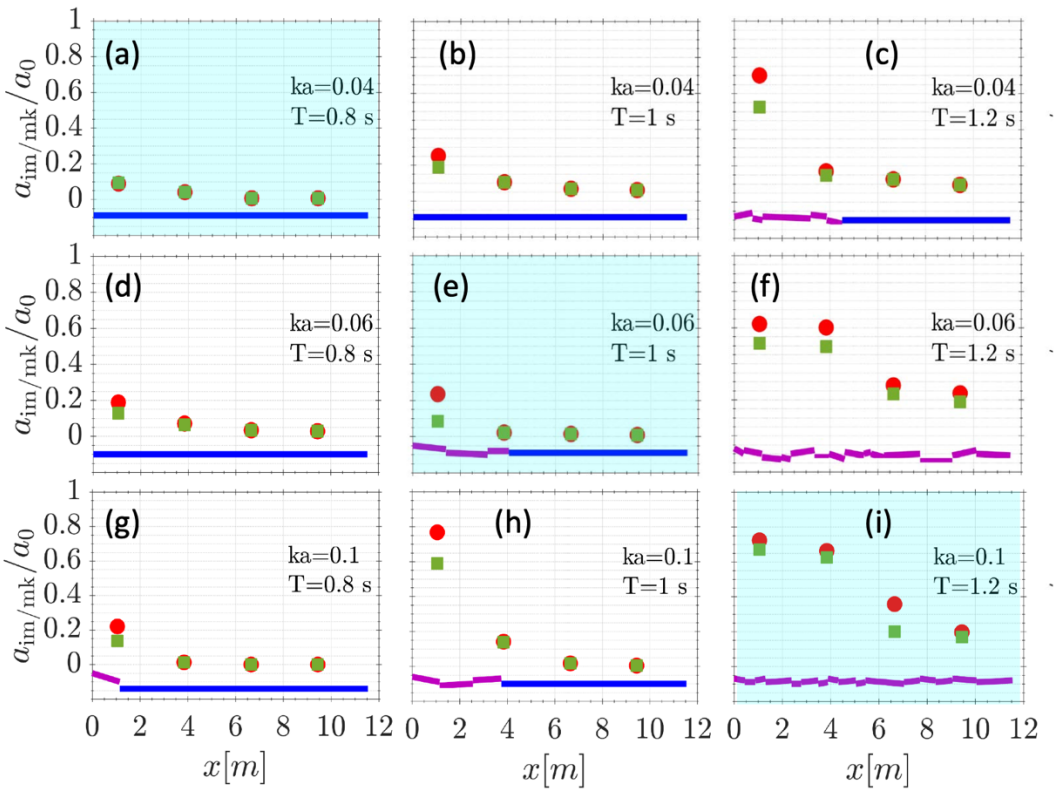

Figure 2: Mean ice (green filled square) and wave/ice-air interface (red filled circle) amplitudes as a function of distance from the wave maker. The continuous (blue thick line) and jagged (pink thick line) lines at the bottom of panels indicate the unbroken and broken status of the ice cover, respectively, at end of each tests; the lengths of broken ice floes are the measured dimension, while vertical displacements are arbitrary.

For the least steep and shortest period incident wave tested, ka = 0.04 and t = 0.8 s, the ice surface undulates with waves and the overwash is shallow, meaning that the amplitudes obtained from the image processing (a_{im}) and the markers in the ice cover (a_{mk}) are identical. The amplitudes are reduced significantly at the first observation point compared with the incident wave amplitude, with $a_{im}/a_0 \approx a_{mk}/a_0 \approx 0.09$. It then reduces steadily along the tank, with $a_{im}/a_0 \approx a_{mk}/a_0 \approx 0.01$ at the last observation point and without breaking the ice.

For the larger steepness, ka = 0.06 in fig. 2(d), the overwash is deeper, and the amplitude a_{im} is slightly greater than a_{mk} at the first observation point. The reduction at the first observation point is less than for the smallest steepness, but nonetheless significant, with $a_{im}/a_0 \approx 0.19$, which is ≈1.5 times greater than a_{mk}/a_0. Moreover, the reduction along the ice cover is rapid so that, at the last observation point, $a_{im}/a_0 \approx 0.03$. The waves do not break the ice but do produce a crack approximately half way along the ice cover.

For the largest steepness, ka = 0.1 in Fig. 2(g), the ice breaks close to its leading edge after 5 s, creating a 1.15 m-long floe, i.e., slightly greater than the incident wavelength. The wave amplitude at the first observation point, in the vicinity of the wave-induced breakup, is larger than for the smaller steepness, with $a_{im}/a_0 \approx 0.22$, which is ≈1.6 times greater than a_{mk}/a_0, due to the presence of overwash. Note that the large bending moments induced by the wave motion cause breakup, while the increase of overwash depth is a consequence of breakup rather than a cause. The amplitudes measured at the subsequent observation points, in the continuous ice cover, are significantly reduced, with $a_{im}/a_0 \approx 0.01$, 0.00, and 0.00, respectively.

For the intermediate wave period, T = 1 s, the two steepest incident waves, ka = 0.06 in Fig. 2(E) and 0.1 in Fig. 2(F), break the ice into multiple floes at the leading edge, over a distance slightly greater than two incident wavelengths. The breakup for ka = 0.06 is relatively slow in comparison to ka = 0.1, for which the breakup occurs in <10 s, i.e., 10 wave periods. For all steepnesses, the amplitudes are greater than in the corresponding tests with the shortest period, particularly at the first observation point where the increase is up to a factor of 3.5 (for the largest steepness). Amplitudes a_{im} are 1.3, 2.8, and 1.3 times larger than the a_{mk} for ka = 0.04, 0.06, and 0.1, respectively. For all steepnesses, by the third observation point, $a_{im}/a_0 < 0.10$ and by the fourth observation point, $a_{im}/a_0 \approx 0.06$.

For the longest incident period, T = 1.2 s, the extent of wave-induced breakup significantly increases. For even the smallest steepness, ka = 0.04 in Fig. 2(c), and ice is broken for ≈2/5 of the ice cover, i.e., slightly greater than two incident wavelengths. The first floe broke away from the edge after <5 s ≈ 4 T, but the next breaking event did not occur until ≈30 s = 25 T. Between the first two breaking events, the overwash reaches the second observation point so that the overwash amplitude is slightly larger there.

The two steepest waves, ka = 0.06 and 0.1 in Figs. 2(F) and 2(I), respectively, break up the entire ice cover, and the breakup reached the far end of the ice cover after only 5–10 s (≈ 4–9 wave periods), noting that further breakup occurred following this. The wave amplitudes at the second, third, and fourth observation points are substantially greater than the smallest steepness case, with the amplitudes at the second observation point similar to those at the first observation point, and non-negligible amplitudes, $a_{im}/a_0 > a_{mk}/a_0 > 0.15$, at the fourth observation point. Moreover, the overwash was intense, getting deeper as the tests progressed, generally ≈30 mm but up to 50 mm, and reaching the fourth observation point after ≈ 40 s. The overwash depth is up to 5 times the ice thickness and ≈1.5 times the incident amplitude, a ≈ 35 mm.

4. AN EXPERIMENTAL MODEL WITH MODEL ICE IN A LARGER FACILITY

The experiments described in Sections 2 and 3 are affected by a number of limitations. These include the use of fresh water ice, which is a more brittle form of ice than the natural sea ice, and two-dimensional physics, which does not describe the full extent of ice break up and thus ice response. To achieve a better understanding of wave-ice interaction, the large wave-ice tank at Aalto University will be accessed within the framework of Hydralab+. The tank is 40 m wide and 40 m long and it is equipped with a directional wave maker at one side and a beach at the other (the basin has been recently refurbished). The advantage of this facility is the availability of model ice, which is a property-controlled material generated by “doping” the water surface with a concentration of ethanol (mechanical properties of ice depends on ethanol concentration), and the large dimensions, which allow ice to break in more natural manner. The experiment will consist of tracing the attenuation rate of incident regular and irregular waves with varying dominant periods and amplitudes and monitoring the concurrent, wave-induced ice breakup.

The initial set up will be a continuous ice sheet with thickness of 0.02m, covering the entire basin. About one third of the ice cover in front of the wave maker will be used to measure mechanical properties using destructive tests and it will be be removed before running the tests. An operational ice surface covering two third of the tank (see figure 3) allows enough space to monitor the incident wave in open water, while leaving enough space for assessing the propagation of waves in ice. Wave propagation and transformation will be monitored in terms of water surface elevation at different distances from the wave maker, using five pressure sensors. The advantage of the pressure sensors is that they are below the water surface and thus are not subjected to collision with ice floes, which would otherwise happen with standard surface sensors. The response of the ice cover will be measured with motion sensors that will be distributed evenly on the surface (see figure 3). Infrared cameras will track the instantaneous positions of the sensors and return their accelerations. The instrumentation is complemented with an industrial camera to monitor the temporal evolution of the ice break up and statistical distribution of the ice floe size distribution.

Tests will run with different initial regular and irregular wave configurations. Wave periods will be T = 1.4, 1.6, and 1.8 s (wavelengths of 3, 4 and 5 m). The wave amplitude will be chosen to have wave steepness ka = 0.08, where k is the wavenumber associated to the wave period and a is the wave amplitude defined as half the wave height. The irregular wave fields defined by a JONSWAP spectral form (Komen et al. 1994), with peak period identical to the period selected for monochromatic waves and significant wave height to ensure an average wave steepness of 0.08. Each test will last 1 hour to allow the ice floe distribution to reach a steady condition. This large run time will allow an estimation of the temporal evolution of wave attenuation as a function of the extent of ice break up and the evaluation of the temporal evolution of floe size distribution.

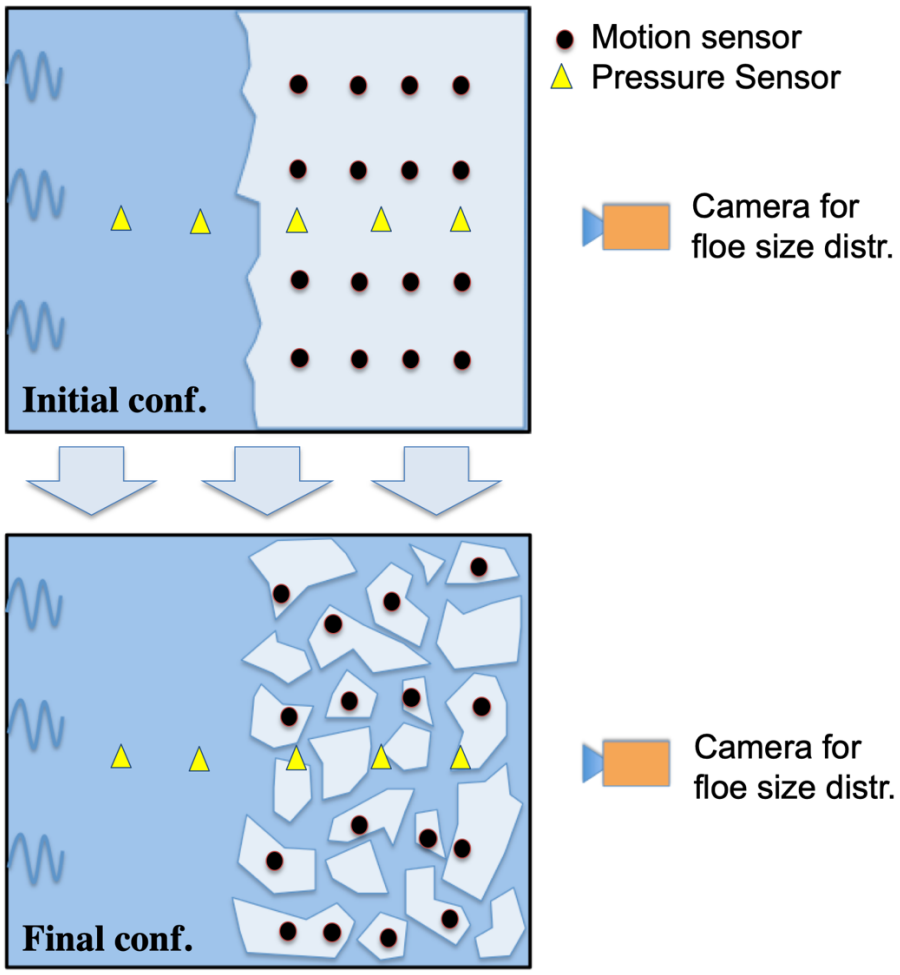

Figure 3: Schematic of the experimental set up in the wave-ice tank at Aalto University

4. CONCLUSIONS

Preparatory tests in a small scale wave-ice flume are reported to explore the interaction between waves and a compact sheet of freshwater ice. Results show that short-period small-steepness incident waves travel only a short distance into the ice-covered water without breaking the ice. As the incident waves get longer and steeper, the waves propagate farther into the ice cover and rapidly break up the ice cover over an increasing distance. Consequently, a sharp transition was noted to rapid breakup of the entire ice cover and wave propagation along the full length of ice-covered water, indicating the existence of a positive feedback loop between increased breakup and increased propagation. Results from this pilot project are limited by the brittle properties of the freshwater ice and the small dimensions of the flume. An experimental model in the large wave-ice tank at Aalto University is planned to validate preliminary results.

ACKNOWLEDGEMENT

This project has received funding from the European Union's Horizon 2020 research and innovation programme under grant agreement No 654110, HYDRALAB+. The authors thank Prof Jason Monty for providing access to the facility at the University of Melbourne. A.T. acknowledge support from the Air-Sea-Ice Lab Project.

REFERENCES

Asplin, M. G., Galley, R., Barber, D. G. and Prinsenberg, S. (2012). Fracture of summer perennial sea ice by ocean swell as a result of Arctic storms. *J. Geophys. Res.* 117 (C06025).

Bennetts, L. G., Alberello, A., Meylan, M. H., Cavaliere, C., Babanin, A. V. and Toffoli, A.

(2015). An idealised experimental model of ocean surface wave transmission by an ice floe. *Ocean Modelling* 96, 85–92.

Bennetts, L. G. and Williams, T. D. (2015). Water wave transmission by an array of floating discs. *Proc. R. Soc. A* 471 (2173), 20140698.

Dolatshah, A., Nelli, F., Bennetts, L.G., Alberello, A., Meylan, M.H., Monty, J.P., Toffoli, A. (2018). Hydroelastic interactions between water waves and floating freshwater ice. *Physics of Fluids*, 30(9), 091702.

Khon, V. C., Mokhov, I. I., Pogarskiy, F. A., Babanin, A., Dethloff, K., Rinke, A., Matthes,
H. (2014). Wave heights in the 21st century Arctic Ocean simulated with a regional climate model. *Geophys. Res. Lett.* 41, 2956–2961.

Kohout, A. L., Williams, M. J. M., Dean, S. M. and Meylan, M. H. 2014 Storm-induced sea ice breakup and the implications for ice extent. Nature pp. 604–607.

Komen, G. J., Cavaleri, L., Donelan, M., Hasselmann, K., Hasselmann, H., Janssen, P. A. E. M. (1994). Dynamics and Modelling of Ocean Waves. *Cambridge University Press*.

Liu, A. K., Mollo-Christensen, E. (1988). Wave propagation in a solid ice pack. *J. Phys. Oceanogr*. 18 (11), 1702–1712.

Masson, D., LeBlond, P. H. (1989). Spectral evolution of wind-generated surface gravity waves in a dispersed ice field. *J. Fluid Mech.* 202, 43–81.

Meylan, M. H., Bennetts, L. G., Kohout, A. L. (2014). In-situ measurements and analysis of ocean waves in the Antarctic marginal ice zone. *Geophys. Res. Lett*. 41, 5046–5051.

Richter-Menge, J., Walsh, J. E., Thomas, K. (2012). Seasonal-to-decadal predictions of Arctic Sea Ice: Challenges and strategies. Tech. Rep. Polar Research Board, National Academy of Sciences, ISBN: 978-0-309-26526-3.

Shen, H. H., Hibler, W. D., Lepparanta, M. (1987). The role of floe collisions in sea ice rheology. *J. Geophys. Res*. 92 (C7), 7085–7096.

Thomson, J., Rogers, W. E. (2014). Swell and sea in the emerging Arctic Ocean. *Geophys. Res. Lett.* 41, 3136–3140.

Toffoli, A., Bennetts, L. G., Meylan, M. H., Cavaliere, C., Alberello, A., Elsnab, J., Monty, J. P. (2015) Sea ice floes dissipate the energy of steep ocean waves. *Geophys. Res. Lett*. 42 (20), 8547–8554.

Wadhams, P. (1983) A mechanism for the formation of ice edge bands. *J. Geophys. Res*. 88 (C5), 2813–2818.

Wadhams, P., Gill, A. E., Linden, P. F. (1979). Transects by submarine of the east Greenland polar front. Deep Sea Research Part A. *Oceanographic Research Papers* 26 (12), 1311–1327.

Wadhams, P., Squire, V. A., Goodman, D. J., Cowan, A. M., Moore, S. C. (1988). The attenuation rates of ocean waves in the marginal ice zone. *J. Geophys. Res*. 93 (C6), 6799–6818.

Wang, R., Shen, H. (2010). Gravity waves propagating into an ice-covered ocean: A viscoelastic model. *J. Geophys. Res.* 115 (C06024).

Williams, T. D., Bennetts, L. G., Dumont, D., Squire, V. A., Bertino, L. (2013). Wave-ice interactions in the marginal ice zone. Part 1: Theoretical foundations. *Ocean Model.* 71, 81–91..